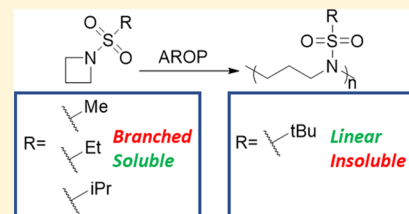


# Comparison of the Anionic Ring-Opening Polymerizations of *N*-(Alkylsulfonyl)azetidines

Elizabeth A. Rowe,<sup>II,‡</sup> Louis Reisman,<sup>II,‡,§</sup> Jennifer A. Jefcoat,<sup>†</sup> and Paul A. Rupar\*,<sup>II,§</sup><sup>II</sup>Department of Chemistry and Biochemistry, The University of Alabama, Tuscaloosa, Alabama 35487-0336, United States<sup>†</sup>U.S. Army Engineer Research and Development Center (ERDC), 3909 Halls Ferry Road Vicksburg, Mississippi 39180, United States

## Supporting Information

**ABSTRACT:** *N*-sulfonylazetidines undergo anionic ring-opening polymerization (AROP) to form poly(*N*-sulfonylazetidine)s, which are potential precursors to valuable polyimines. In this work, the impacts of alkyl sulfonyl substitution on the AROP of (*N*-(ethanesulfonyl)azetidine (EsAzet), *N*-(2-propanesulfonyl)azetidine (iPsAzet), and *N*-(*tert*-butylsulfonyl)azetidine (tBsAzet) are studied and compared to those of the previously reported polymerization of *N*-(methanesulfonyl)azetidine (MsAzet). The polymerization kinetics of EsAzet and iPsAzet is of the first order with respect to their monomers and produces p(EsAzet) and p(iPsAzet), which are both soluble in DMF and DMSO. In contrast, the polymerization of tBsAzet proceeds only to low conversion due to precipitation of p(tBsAzet) under identical conditions. At lower temperatures (120 °C), iPsAzet polymerizes with the fastest rate, while at higher temperatures (180 °C), the rate of MsAzet is the fastest. The reordering of the relative polymerization rates of MsAzet, EsAzet, and iPsAzet occurs due to the interplay of the Arrhenius frequency factors and the Arrhenius activation energies of each system. The difference in the solubility of p(EsAzet) and p(iPsAzet) compared to p(tBsAzet) occurs because the polymer chains of p(EsAzet) and p(iPsAzet) have branched structures, whereas those of p(tBsAzet) are linear. The branched structures of p(EsAzet) and p(iPsAzet) arise due to chain transfer by deprotonation of the  $\alpha$ -sulfonyl protons and nucleophilic addition of the resulting methanide anion to subsequent monomers during the polymerization.



## INTRODUCTION

Although there are structural similarities between strained cyclic oxides and cyclic imines, they have very different polymerization chemistries. While cyclic oxides can polymerize by various mechanisms<sup>1–3</sup> to produce linear polymers with high degrees of control, cyclic imines only polymerize via cationic ring-opening polymerization (CROP) to produce hyperbranched polymers (Scheme 1A).<sup>4–9</sup> This lack of control has led to indirect routes to produce polyimines, most notably, the polymerizations of oxazolines and oxazines, despite the difficulties associated with these approaches.<sup>5,10–21</sup> However, the high-value applications of polyimines in antimicrobial and antifouling coatings,<sup>22</sup> chelation and polymer-assisted deposition,<sup>23</sup> CO<sub>2</sub> capture,<sup>8,9,24–27</sup> and nonviral gene transfection<sup>5</sup> make novel controlled routes to polyimines highly desirable.

In 2005, Bergmann and Toste<sup>28</sup> reported the anionic ring-opening polymerization (AROP) of *N*-sulfonyl-2-methylaziridines. This was a significant breakthrough as the resulting polymers could be converted to linear polypropylenimine and thus represented the first example of a living AROP route to polyimines (Scheme 1B). Since this initial report, Wurm et al.,<sup>29–39</sup> Taton et al.,<sup>40–42</sup> Guo et al.,<sup>43</sup> Zhang and Wu,<sup>44</sup> and we ourselves<sup>45,46</sup> have studied the polymerization of numerous *N*-sulfonylaziridines and their subsequent deprotection to afford linear polyimines.<sup>47</sup>

In efforts to synthesize linear poly(trimethylenimine) (LPTMI) via an AROP route, we recently reported the

AROP of *N*-(methanesulfonyl)azetidine (MsAzet) (Scheme 1C). Surprisingly, the resulting p(MsAzet) had a branched structure as opposed to the anticipated linear structure.<sup>48</sup> Branching occurred due to deprotonation of the methanesulfonyl group<sup>49</sup> during the course of the polymerization and subsequent chain initiation from the methanide anion. The chain-transfer mechanism appears to be a consequence of the high temperature required for the AROP of MsAzet (>120 °C) as branching has not been detected in the lower-temperature AROP of *N*-(methanesulfonyl)aziridines (<50 °C).<sup>29,33–35,39,44,45,47</sup>

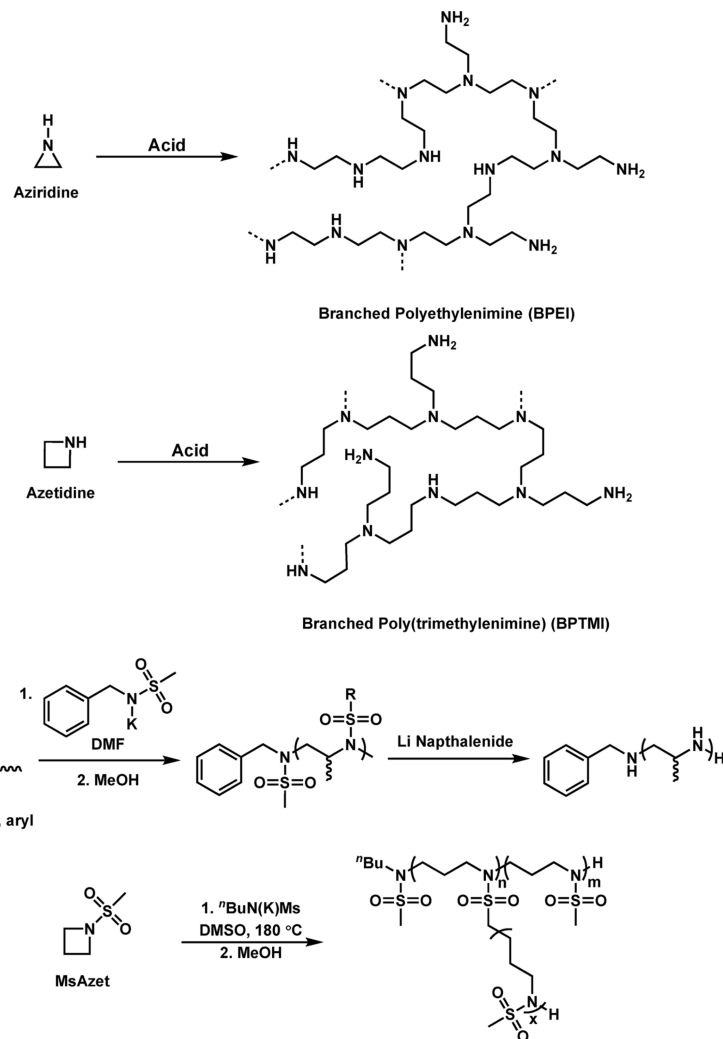
In attempts to prevent the branching observed during the polymerization of MsAzet, we explored the copolymerization of *N*-(*o*-tolylsulfonyl)azetidine (*o*TsAzet) and *N*-(*p*-tolylsulfonyl)azetidine (*p*TsAzet), which both lack protons  $\alpha$  to the sulfonyl.<sup>50</sup> The copolymerization of two *N*-(tolylsulfonyl)azetidines produced linear copolymers with narrow dispersities, and the resulting polymer could be converted to LPTMI. Copolymerization of the two monomers was required due to the insolubility of the polymers formed from homopolymerizations of *o*TsAzet and *p*TsAzet.

In this report, three *N*-(alkylsulfonyl)azetidines, *N*-(*tert*-butylsulfonyl)azetidine (tBsAzet), *N*-(2-propanesulfonyl)-

Received: July 12, 2019

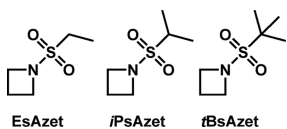
Revised: September 26, 2019

Published: October 16, 2019

Scheme 1. Ring-Opening Polymerizations of aziridines and azetidines<sup>a</sup>

<sup>a</sup>(A) CROP of aziridine and azetidine. (B) AROP of *N*-sulfonyl-2-methylaziridine reported by Bergmann and Toste.<sup>28</sup> (C) AROP of MsAzet.<sup>48</sup>

azetidine (*i*PsAzet), and *N*-(ethanesulfonyl)azetidine (EsAzet), were studied (Chart 1). *t*BsAzet is incapable of branching

Chart 1. *N*-(alkylsulfonyl)azetidines.

through the mechanism observed for MsAzet and therefore should produce only linear *p*(*N*-sulfonylazetidine). Additionally, the *tert*-butylsulfonyl group is readily removed under mild acidic conditions,<sup>51</sup> thus potentially providing easy access to LPTMI from a *t*BsAzet-derived polymer.<sup>50</sup> For *i*PsAzet and EsAzet, we proposed that the increased sterics and electron richness at the sulfonyl  $\alpha$  carbon may reduce or inhibit the branching reactions observed in MsAzet polymerizations. While the polymers produced from *i*PsAzet are linear, surprisingly, the polymers produced from EsAzet are branched more so than those of *p*(MsAzet).

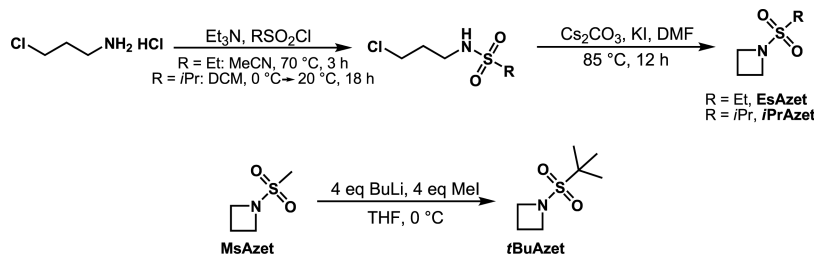
## MATERIALS AND METHODS

All manipulations were carried out under an anhydrous N<sub>2</sub> atmosphere using standard Schlenk line and glovebox techniques. Solvents were purified by passing through an alumina column, degassed, and then stored over 3 Å molecular sieves. Size exclusion chromatography (SEC) was performed using a Malvern Viscotek gel permeation chromatograph equipped with an RI detector, an automatic sampler, a pump, an injector, an inline degasser, a column oven (60 °C), and two in-series Malvern T6000 M SEC columns. DMF was used as the mobile phase at a flow rate of 1 mL/min.

<sup>1</sup>H NMR end-group analysis was performed by comparing the integration of the CH<sub>3</sub> group of the <sup>7</sup>BuN<sub>3</sub> or <sup>7</sup>BuNMs chain end to the methylene signals of the polymer backbone.

MALDI-TOF mass spectra were acquired on a Bruker rapifleX MALDI-TOF mass spectrometer. The polymer MALDI-TOF mass spectra were acquired in the reflectron positive mode, and samples were prepared using the dried-droplet method. Briefly, 2  $\mu$ L of the polymer (10 mg/mL) in DMF was mixed with 10  $\mu$ L of DHB (10 mg/mL) in THF and 1  $\mu$ L of NaI (10 mg/mL) in THF. One microliter of this solution was spotted and allowed to dry.

DSC analysis was performed on a TA DSC250 with a heating/cooling rate of 10 °C/min. For the DSC data collection, all samples were heated through two complete heating/cooling cycles. The data from the second cycle is reported. TGA analysis was performed on a Netzsch STA 449 F1 Jupiter with a heating rate of 10 °C/min.

Scheme 2. Synthesis of EsAzet, iPsAzet, and tBsAzet<sup>a</sup>

<sup>a</sup>Top: synthesis of EsAzet and iPsAzet and bottom: synthesis of tBsAzet.

MsAzet and *N*-(ethanesulfonyl)azetidine (EsAzet) were synthesized based on the literature procedure and were purified via two sublimations (the first over  $\text{CaH}_2$ ) at 60 °C and 50 mTorr.<sup>48</sup>

<sup>"</sup>BuN(H)*p*Ts<sup>50</sup> and <sup>"</sup>BuN(H)Ms<sup>28</sup> initiators were synthesized based on the literature procedure and were purified by distillation at 120 °C and 50 mTorr.

**N-(3-Chloropropyl)propane-2-sulfonamide.** To 3-chloropropylamine hydrogen chloride (6.20 g, 47.7 mmol) and triethylamine (12.9 mL, 92.3 mmol) in DCM (300 mL) at 0 °C was added 2-propanesulfonyl chloride (5.18 mL, 46.1 mmol). The solution was stirred for 18 h, and during which it warmed to room temperature. Brine (250 mL) was added, and the solution was then extracted with DCM (3 × 400 mL). The combined organic layers were washed with aqueous 1 M HCl (100 mL), water (100 mL), dried over  $\text{MgSO}_4$ , and condensed to afford a clear, colorless oil (5.36 g, 58.2%).

<sup>1</sup>H NMR (600 MHz,  $\text{CDCl}_3$ ):  $\delta$  1.36 (d, 6H,  $\text{CH}-(\text{CH}_3)_2$ ), 2.02 (quint, 2H,  $\text{CH}_2\text{-CH}_2\text{-CH}_2$ ), 3.17 (sep, 1H,  $\text{CH}-(\text{CH}_3)_2$ ), 3.30 (q, 2H,  $\text{CH}_2\text{-CH}_2\text{-N}$ ), 3.63 (t, 2H,  $\text{CH}_2\text{-Cl}$ ), 4.67 (br, 1H, NH) (Figure S1).

<sup>13</sup>C NMR (125 MHz,  $\text{CDCl}_3$ ):  $\delta$  16.71, 33.26, 40.89, 41.91, 53.47 (Figure S2).

HRMS:  $[\text{M}^+] = 199.0434$  (theoretical), 199.0440 (observed).

Anal. calcd for  $\text{C}_6\text{H}_{14}\text{ClNO}_2\text{S}$  (199.0434 g/mol): C, 36.09; H, 7.07; N, 7.01; found: C, 36.33; H, 6.92; N, 6.88.

**N-(2-Propanesulfonyl)azetidine (iPsAzet).** iPsAzet was synthesized by adapting the procedure of Reibenspies, et al.<sup>52</sup> To *N*-(3-chloropropyl)propane-2-sulfonamide (5.20 g, 26.0 mmol) in DMF (200 mL) was added  $\text{Cs}_2\text{CO}_3$  (15.0 g, 42.5 mmol) and KI (8.10 g, 48.8 mmol). The mixture was heated to 95 °C in open air for 18 h. After cooling to room temperature, the solvent was removed. To the off-white solid was added brine (100 mL) and DCM (300 mL) and extracted two additional times with DCM (2 × 300 mL). The combined organic layers were washed with water (100 mL), dried over  $\text{MgSO}_4$ , and condensed to afford a thick brown oil. This oil was purified by distillation over  $\text{CaH}_2$  at 50 °C and 50 mTorr to afford a clear, colorless oil (2.08 g, 48.9%).

<sup>1</sup>H NMR (600 MHz,  $\text{DMSO-d}_6$ ):  $\delta$  1.20 (d, 6H,  $\text{CH}-(\text{CH}_3)_2$ ), 2.20 (quint, 2H,  $\text{CH}_2\text{-CH}_2\text{-CH}_2$ ), 3.20 (sep, 1H,  $\text{CH}-(\text{CH}_3)_2$ ), 3.84 (t, 4H,  $\text{CH}_2\text{-CH}_2\text{-N}$ ) (Figure S3).

<sup>13</sup>C NMR (125 MHz,  $\text{CDCl}_3$ ):  $\delta$  15.47, 16.46, 50.93, 53.46 (Figure S4).

HRMS:  $[\text{M}^+] = 163.0667$  (theoretical), 163.0661 (observed).

Anal. calcd for  $\text{C}_6\text{H}_{13}\text{NO}_2\text{S}$  (163.0667 g/mol): C, 44.15; H, 8.03; N, 8.58; found: C, 44.41; H, 8.26; N, 8.72.

**N-(tert-Butylsulfonyl)azetidine (tBsAzet).** MsAzet (100 mg, 0.740 mmol) in THF (4 mL) was cooled to 0 °C, and 1.6 M BuLi (0.46 mL, 0.736 mmol) was added slowly followed by MeI (0.05 mL, 0.803 mmol). The reaction was then stirred for 15 min at 0 °C. This was repeated an additional time with 1.6 M BuLi (0.46 mL, 0.736 mmol) and MeI (0.05 mL, 0.803 mmol). To the reaction was then added 1.6 M BuLi (0.95 mL, 1.52 mmol) and MeI (0.10 mL, 1.61 mmol) and stirred for 1 h at 0 °C. The reaction was then quenched with brine (10 mL) and extracted with DCM (3 × 20 mL). The combined organic layers were dried over  $\text{MgSO}_4$  and condensed to afford a clear, yellow oil. This yellow oil was purified by column chromatography on basic alumina with DCM as the mobile phase to

produce a clear, colorless oil. This oil was dried by distillation over  $\text{CaH}_2$  at 50 °C and 50 mTorr to afford a clear, colorless oil (66.9 mg, 51.0%). Note: there is a small impurity in tBsAzet that could not be removed and is believed to arise because of deprotection of the *tert*-butylsulfonyl group.<sup>51</sup>

<sup>1</sup>H NMR (600 MHz,  $\text{CDCl}_3$ ):  $\delta$  1.35 (s, 9H,  $\text{C}-(\text{CH}_3)_3$ ), 2.26 (quint, 2H,  $\text{CH}_2\text{-CH}_2\text{-CH}_2$ ), 4.00 (t, 4H,  $\text{CH}_2\text{-CH}_2\text{-N}$ ) (Figure S5).

<sup>13</sup>C NMR (125 MHz,  $\text{CDCl}_3$ ):  $\delta$  15.47, 24.13, 51.78, 59.59 (Figure S6).

HRMS:  $[\text{M}^+] = 177.0824$  (theoretical), 177.0816 (observed).

**Polymerizations.** All polymerizations were performed using the same procedure except that the monomer to initiator ratio and the monomer used were varied. The procedure below is for a polymer with a target  $[\text{M}]:[\text{I}]$  of 40:1.

A stock solution of <sup>"</sup>BuN(K)Ts in anhydrous DMF was prepared by combining potassium hexamethyldisilazide (KHMDS) (54 mg, 0.27 mmol) and *N*-butyl-*N*-*p*-toluenesulfonamide (<sup>"</sup>BuN(H)Ts) (62 mg, 0.27 mmol) in DMF (2 mL). This solution was stirred for 1 h at room temperature. The resulting solution of <sup>"</sup>BuN(K)Ts in DMF was used without any further characterization or purification.

To anhydrous DMF (0.60 mL) was added the monomer (0.44 mmol). To this solution was added a portion of the prepared <sup>"</sup>BuN(K)Ts DMF (0.08 mL, 0.011 mmol). The reaction mixture was then heated to 120 °C for 19 days. After this time, the reaction was then precipitated into water (15 mL), collected by centrifugation, and dried overnight under vacuum at 100 °C. Characterization of the polymers is below:

*p*(MsAzet): brown amorphous glass (45.8 mg, 76.3% isolated yield,  $M_n$  (RI, SEC vs PS standards) = 10.6 kDa,  $D = 1.06$ , target  $D_p = 40$ , actual  $D_p$  (<sup>1</sup>H NMR) = 33). See Figure S21 for the SEC trace.

<sup>1</sup>H NMR (Figure S7) and <sup>13</sup>C NMR matched the literature.<sup>48</sup>

MALDI-TOF MS: See Figure S16.

*p*(EsAzet): brown amorphous glass (53.7 mg, 81.4% isolated yield,  $M_n$  (RI, SEC vs PS standards) = 9.82 kDa,  $D = 1.09$ , target  $D_p = 40$ , actual  $D_p$  (<sup>1</sup>H NMR) = 33). See Figure S21 for the SEC trace.

<sup>1</sup>H NMR (600 MHz,  $\text{DMSO-d}_6$ ):  $\delta$  0.89 (t,  $\text{CH}_2\text{-CH}_3$ ), 1.20 (t,  $\text{SO}_2\text{-CH}_2\text{-CH}_3$ ), 1.43 (m,  $\text{CH}_2\text{-CH}_2\text{-CH}_2\text{-CH}_3$ ), 1.80 (br,  $\text{CH}_2\text{-CH}_2\text{-CH}_2\text{-N}$ ), 2.39 (s, Ar- $\text{CH}_3$ ), 3.05 (q,  $\text{SO}_2\text{-CH}_2\text{-CH}_3$ ), 3.17 (t,  $\text{CH}_2\text{-CH}_2\text{-N}$ ), 7.00 (t, NH), 7.41 (d, Ar), 7.66 (d, Ar) (Figures S8 and S9).

<sup>13</sup>C NMR (125 MHz,  $\text{DMSO-d}_6$ ):  $\delta$  7.80, 28.07, 44.72, 45.17 (Figure S10).

MALDI-TOF MS: See Figures S14 and S17.

*p*(iPsAzet): brown amorphous glass (55.3 mg, 76.8% isolated yield,  $M_n$  (RI, SEC vs PS standards) = 8.65 kDa,  $D = 1.08$ , target  $D_p = 40$ , actual  $D_p$  (<sup>1</sup>H NMR) = 33). See Figure S21 for the SEC trace.

<sup>1</sup>H NMR (600 MHz,  $\text{DMSO-d}_6$ ):  $\delta$  0.85 (t,  $\text{CH}_2\text{-CH}_3$ ), 1.20 (d,  $\text{SO}_2\text{-CH}_2\text{-CH}_3$ ), 1.43 (m,  $\text{CH}_2\text{-CH}_2\text{-CH}_2\text{-CH}_3$ ), 1.80 (br,  $\text{CH}_2\text{-CH}_2\text{-CH}_2\text{-N}$ ), 2.39 (s, Ar- $\text{CH}_3$ ), 3.20 (t,  $\text{CH}_2\text{-CH}_2\text{-N}$ ), 3.30 (q,  $\text{SO}_2\text{-CH}_2\text{-CH}_3$ ), 6.97 (t, NH), 7.41 (d, Ar), 7.66 (d, Ar) (Figures S11 and S12).

<sup>13</sup>C NMR (125 MHz,  $\text{DMSO-d}_6$ ):  $\delta$  16.36, 28.17, 45.24, 52.04 (Figure S13).

MALDI-TOF MS: See Figures S15 and S18.

**Kinetic Studies of the Polymerizations of EsAzet and iPsAzet.** All kinetic studies were performed using the above procedure except that the solvent used was  $\text{DMSO-d}_6$  and the

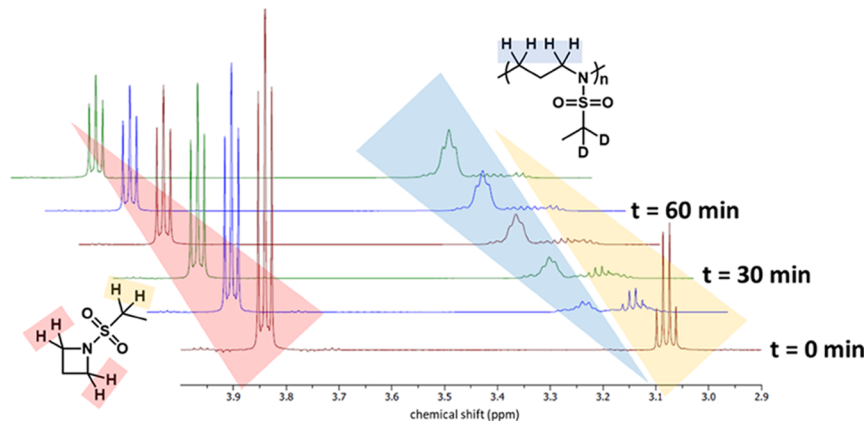


**Figure 1.** Progress of EsAzet polymerization as monitored by real-time  $^1\text{H}$  NMR spectroscopy in  $\text{DMSO}-d_6$  at  $160\text{ }^\circ\text{C}$ . Note: H-D exchange occurs at the sulfonyl  $\alpha$  carbon (yellow).

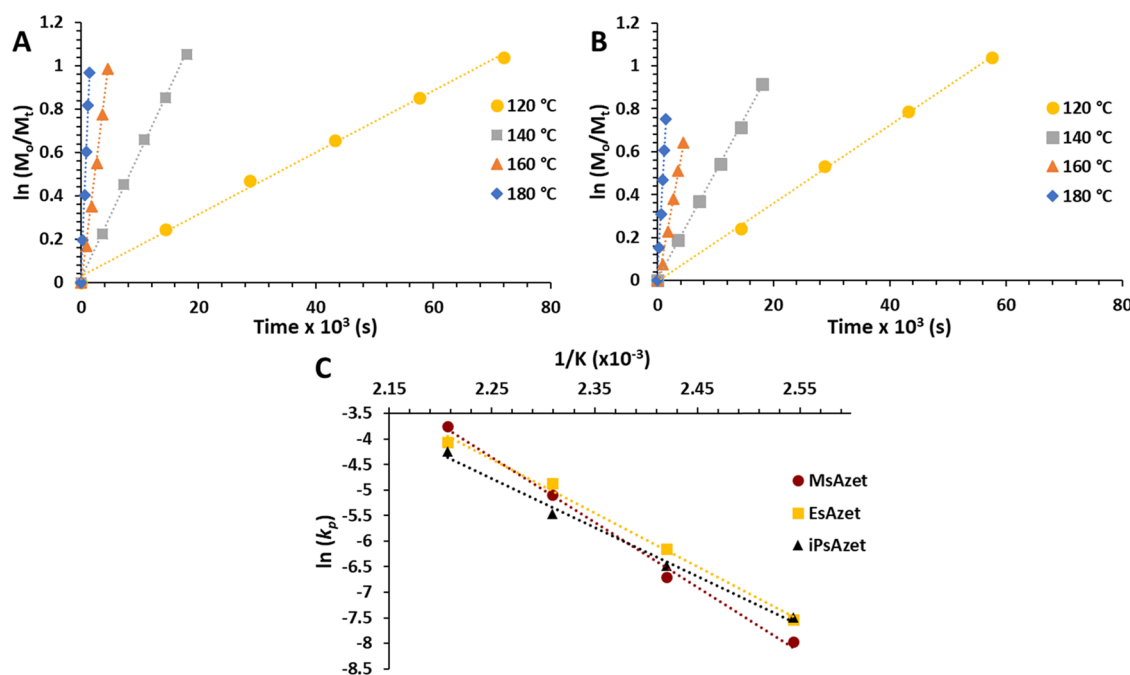


**Figure 2.**  $\ln([M_0]/[M_t])$  vs time for the AROP of (A) EsAzet and (B) *i*PsAzet in  $\text{DMSO}-d_6$  with a  $[M_0]:[I_0]$  of  $\sim 20:1$  at temperatures ranging from  $120$  to  $180\text{ }^\circ\text{C}$ . (C) Arrhenius plots constructed with data in Table 1. The data for the polymerization of MsAzet comes from ref 48.

temperature of the reaction varied. All polymerizations were monitored until a conversion of  $\geq 60\%$  was achieved. A monomer: initiator ratio of  $\sim 20:1$  was used, and  $^1\text{H}$  NMR spectra were recorded as follows:  $120\text{ }^\circ\text{C}$  (every 4 h),  $140\text{ }^\circ\text{C}$  (every 1 h),  $160\text{ }^\circ\text{C}$  (every 15 min), and  $180\text{ }^\circ\text{C}$  (every 5 min).

## RESULTS AND DISCUSSION

**Monomer Synthesis and Initial Polymerization Studies.** EsAzet and *i*PsAzet were synthesized using conditions similar to those used to synthesize MsAzet.<sup>48,52</sup> *t*BsAzet was synthesized from MsAzet via sequential deprotonations of the sulfonyl group with  $\text{BuLi}$  followed by reaction with  $\text{MeI}$  (Scheme 2). The motivation for synthesizing EsAzet and *i*PsAzet as monomers is that the increased substitution at the sulfonyl  $\alpha$  carbon should make deprotonation less favored due to electronic and steric influences and therefore could suppress branching compared to MsAzet. *t*BsAzet is an appealing monomer as there are no protons  $\alpha$  to the sulfonyl, so

activation and thus branching cannot occur through the mechanism observed with MsAzet.

As with previous work on *N*-sulfonylazetidines,<sup>48,50</sup> polymerizations of the *N*-(alkylsulfonyl)azetidines were performed in polar, aprotic solvents (i.e.,  $\text{DMSO}$ ,  $\text{DMF}$ , and  $\text{NMP}$ ) at temperatures  $\geq 120\text{ }^\circ\text{C}$  in the presence of a deprotonated sulfonamide initiator. In the case of the polymerizations of EsAzet and *i*PsAzet, the resulting *p*(EsAzet) and *p*(*i*PsAzet) were purified by precipitation in water to afford brown amorphous glasses, which are soluble in  $\text{DMF}$  and  $\text{DMSO}$ . *p*(EsAzet) and *p*(*i*PsAzet) have  $T_g$ 's of  $55$  and  $40\text{ }^\circ\text{C}$ , respectively, and are thermally stable up to  $300\text{ }^\circ\text{C}$  (Figures S22–S25). For comparison, *p*(MsAzet) has been previously characterized with a  $T_g$  of  $50\text{ }^\circ\text{C}$  and is thermally stable up to  $300\text{ }^\circ\text{C}$ .<sup>48</sup> Interestingly, *p*(EsAzet) also showed a  $T_m$  and  $T_c$  of  $195\text{ }^\circ\text{C}$  and  $180\text{ }^\circ\text{C}$ , respectively (Figure S22). While the polymers studied in this work are all low molecular weights, higher molecular weights could be achieved by varying the monomer to initiator ratio.<sup>48,50</sup>

Table 1. Summary of the Kinetic Data of *N*-(Alkylsulfonyl)azetidine Polymerizations<sup>a</sup>

| monomer | [M]:[I] | temp (°C) | $k_{app}^b \times 10^{-5}$ (L M <sup>-1</sup> s <sup>-1</sup> ) | $k_p^c \times 10^{-4}$ (M <sup>-1</sup> s <sup>-1</sup> ) | M <sub>n</sub> (kg/mol) |                                 |                | ref       |
|---------|---------|-----------|---|---|-------------------------|---------------------------------|----------------|-----------|
|         |         |           |   |   | SEC <sup>d</sup>        | <sup>1</sup> H NMR <sup>e</sup> | D <sup>d</sup> |           |
| MsAzet  | 22:1    | 120       | 1.01  | 3.45  | 9.40                    | 2.86                            | 1.06           | 48        |
| MsAzet  | 22:1    | 140       | 3.55  | 12.2  | 9.00                    | 2.80                            | 1.06           |           |
| MsAzet  | 22:1    | 160       | 17.9  | 61.3  | 9.40                    | 2.75                            | 1.07           |           |
| MsAzet  | 22:1    | 180       | 68.5  | 235   | 8.30                    | 2.72                            | 1.13           |           |
| EsAzet  | 21:1    | 120       | 1.48  | 5.34  | 9.00                    | 4.38                            | 1.07           | this Work |
| EsAzet  | 21:1    | 140       | 5.94  | 21.4  | 8.60                    | 3.93                            | 1.07           |           |
| EsAzet  | 21:1    | 160       | 21.3  | 76.9  | 7.53                    | 3.80                            | 1.14           |           |
| EsAzet  | 15:1    | 180       | 66.2  | 171   | 5.81                    | 2.10                            | 1.12           |           |
| iPsAzet | 18:1    | 120       | 1.81  | 5.58  | 6.33                    | 3.44                            | 1.09           |           |
| iPsAzet | 18:1    | 140       | 4.98  | 15.3  | 5.95                    | 3.39                            | 1.12           |           |
| iPsAzet | 18:1    | 160       | 13.8  | 42.5  | 5.30                    | 3.36                            | 1.13           |           |
| iPsAzet | 18:1    | 180       | 46.4  | 143   | 4.10                    | 2.61                            | 1.18           |           |

<sup>a</sup>The data for the polymerization of MsAzet comes from ref 48. <sup>b</sup> $k_{app}$  = slope from plot of  $\ln([M_0]/[M_t])$  vs time. <sup>c</sup> $k_p = k_{app}/[I]$ . <sup>d</sup>Determined via SEC vs PS standards. <sup>e</sup>Determined via <sup>1</sup>H NMR spectroscopic end-group analysis.

Interestingly, the polymerization of *t*BsAzet produced an insoluble material, presumed to be p(*t*BsAzet), at low degrees of conversion. Due to the difficulties associated with the characterization of the insoluble material, p(*t*BsAzet) was not further studied. The insolubility of p(*t*BsAzet) is discussed later in this manuscript.

**Kinetic Studies.** The kinetics of EsAzet and iPsAzet polymerizations in DMSO-*d*<sub>6</sub> over a range of temperatures was measured and compared to that of MsAzet.<sup>48</sup> The polymerizations were performed between 120 and 180 °C with a [M]:[I] of ~20:1 and were monitored via real-time <sup>1</sup>H NMR spectroscopy. The extent of polymerization was determined by observing the disappearance of the monomer methylene protons and the appearance of these same protons in the polymer chain (Figure 1). As with polymerizations of MsAzet performed in DMSO-*d*<sub>6</sub>, H–D exchange of the protons  $\alpha$  to the sulfonyl was observed to occur in both EsAzet and iPsAzet polymerizations. This H–D exchange indicates that the increase in alkyl substitution on the sulfonyl does not prevent sulfamoyl methanide formation during the polymerization.

The plots of  $\ln([M_0]/[M_t])$  versus time for the p(EsAzet) and p(iPsAzet) polymerizations are linear (Figure 2A,B) and consistent with the polymerizations being of the first order with respect to monomer concentration and a constant number of active polymer chain ends. Assuming the reaction is of the first order with respect to [I]<sub>0</sub>,<sup>53</sup> the propagation rate constants ( $k_p$ ) for the polymerization of EsAzet and iPsAzet are  $5.34 \times 10^{-4}$  and  $5.58 \times 10^{-4}$  M<sup>-1</sup> s<sup>-1</sup> at 120 °C, respectively (Table 1). Both of these values are higher than the  $k_p$  for the polymerization of MsAzet ( $3.45 \times 10^{-4}$  M<sup>-1</sup> s<sup>-1</sup> at 120 °C) and suggest that increasing alkyl substitution on the sulfonyl increases the rate of polymerization.<sup>48</sup> Interestingly, at 180 °C, the ordering of the  $k_p$  of MsAzet, EsAzet, and iPsAzet reverses such that the rate of polymerization has an arrangement of MsAzet > EsAzet > iPsAzet (Table 2). It is worth noting that the  $k_p$  for the copolymerization of *o*TsAzet and *p*TsAzet is faster than that of the *N*-(alkylsulfonyl)-azetidine monomers studied at both 120 and 180 °C.<sup>50</sup>

For each monomer, Arrhenius plots were constructed using the polymerization rate constants at four different temperatures (Figure 2C). The activation energy ( $E_a$ ) of the monomer decreases with increasing alkyl substitution on the sulfonyl group (MsAzet > EsAzet > iPsAzet) (Table 3). We propose that this is a consequence of increased nucleophilicity

Table 2. Summary of the Trends in Propagation Rate Constants of the AROP of *N*-(Alkylsulfonyl)azetidines<sup>a</sup>

| temp (°C) | trend ( $k_p$ )           |
|-----------|---------------------------|
| 120       | iPsAzet > EsAzet > MsAzet |
| 140       | EsAzet > iPsAzet > MsAzet |
| 160       | EsAzet > MsAzet > iPsAzet |
| 180       | MsAzet > EsAzet > iPsAzet |

<sup>a</sup>The data for the polymerization of MsAzet comes from ref 48.

Table 3. Data Obtained from the Arrhenius Plots of *N*-(Alkylsulfonyl)azetidines<sup>a</sup>

| monomer | activation energy ( $E_a$ ) (kcal/mol) | frequency factor (A) (M <sup>-1</sup> s <sup>-1</sup> ) |
|---------|--|---|
| MsAzet  | 25.2                                   | $3.24 \times 10^{10}$                                   |
| EsAzet  | 20.7                                   | $1.94 \times 10^8$                                      |
| iPsAzet | 19.0                                   | $1.80 \times 10^7$                                      |

<sup>a</sup>The data for the polymerization of MsAzet comes from ref 48.

of the propagating anion due to increasing electron density as the substitution at the sulfonyl  $\alpha$  carbon increase from methyl to ethyl to isopropyl. However, it should be noted that our observations contrast with reports that electron-withdrawing substituents increase the rate of *N*-sulfonylaziridines<sup>34</sup> and that the nucleophilicity of the propagating anion does not play a major role in the polymerization but rather the electrophilicity of the monomer.<sup>39</sup>

The ordering of the Arrhenius frequency factors for the AROP of the monomers is MsAzet > EsAzet > iPsAzet (Table 3). This is likely related to the sterics of the alkyl sulfonyl groups on the monomers and active chain ends. Specifically, the methyl group of MsAzet is the smallest and therefore has the highest frequency factor, whereas the isopropyl group of the iPsAzet is the bulkiest and therefore has the lowest frequency factor. Over all, it is the interplay of the differing polymerization  $E_a$  values and frequency factors (Table 3) of MsAzet, EsAzet, and iPsAzet that leads to a reversal in the ordering of their polymerization rates between 120 and 180 °C (Tables 1 and 2). Eyring plots (Figure S26) of the kinetic data led to similar conclusions with the MsAzet having the highest enthalpy of activation ( $\Delta H^\ddagger$ ) and iPsAzet having the lowest  $\Delta H^\ddagger$  (Table S1). The entropy of activation ( $\Delta S^\ddagger$ ) was found to follow a similar trend to the frequency factor in which the  $\Delta S^\ddagger$

**Table 4. Polymer Characterization Data Comparing the Degree of Branching Using  $^1\text{H}$  NMR Spectroscopic End-Group Analysis**

| monomer | [M]:[I] |                     | M <sub>n</sub> (kg/mol) |                  |                               |                |  |
|---------|---------|---------------------|-------------------------|------------------|-------------------------------|----------------|--|
|         | theor   | actual <sup>b</sup> | theor                   | SEC <sup>a</sup> | $^1\text{H}$ NMR <sup>b</sup> | D <sup>a</sup> | $\omega:\alpha$ ratio <sup>c</sup> (S/N ( $\omega,\alpha$ )) |
| MsAzet  | 40:1    | 33:1                | 5.63                    | 10.6             | 4.71                          | 1.06           | 1.04:3.00 (1418, 6081)                                       |
| EsAzet  | 40:1    | 33:1                | 6.20                    | 9.82             | 5.22                          | 1.09           | 1.10:3.00 (2612, 10,225)                                     |
| iPsAzet | 40:1    | 33:1                | 6.76                    | 8.65             | 5.62                          | 1.08           | 1.23:3.00 (1655, 5405)                                       |

<sup>a</sup>Determined via SEC vs PS standards. <sup>b</sup>Determined via  $^1\text{H}$  NMR spectroscopic end-group analysis. <sup>c</sup>Determined via  $^1\text{H}$  NMR spectroscopic integrations of the signals attributed to the  $\omega$  (terminal sulfonamide; 6.95 ppm) and the  $\alpha$  ("BuNTs methyl protons; 0.89 ppm) chain ends. Signal to noise ratios were calculated for the  $\text{CH}_3$  group on the "BuNTs chain end and the NH chain end using Mestrenova Pro.

becomes more negative with increasing substitution on the sulfonyl group (Table S1) and is consistent with increased sterics leading to a larger entropic barrier in the transition state.

**Evidence of Chain Transfer in the Polymerizations of EsAzet and iPsAzet.** We previously reported that the AROP of MsAzet produces p(MsAzet) with a branched structure with the branching arising as a consequence of deprotonation of the methanesulfonyl during the course of the polymerization.<sup>48</sup> Evidence for the methanide formation during the polymerization of MsAzet came from the observation of rapid H–D exchange at the methanesulfonyl group when polymerizations were conducted in  $\text{DMSO}-d_6$ .

We anticipated that the increased  $\text{pK}_a$  and sterics of the more substituted alkyl groups of EsAzet and iPsAzet could suppress deprotonation and polymer branching. This is not the case as  $^1\text{H}$  NMR spectroscopic monitoring of polymerizations of EsAzet and iPsAzet performed in  $\text{DMSO}-d_6$  showed rapid H–D exchange  $\alpha$  to the sulfonyl in both EsAzet and iPsAzet. H–D exchange at the  $\alpha$ -sulfonyl protons was also evident in the MALDI-TOF mass spectra of p(EsAzet) and p(iPsAzet) samples polymerized in  $\text{DMSO}-d_6$  (Figures S14 and S15).

The fact that H–D exchange is occurring during  $\text{DMSO}-d_6$ -solvated polymerizations of EsAzet and iPsAzet strongly suggests that branching is also occurring. Indeed, branching is supported by  $^1\text{H}$  NMR end-group analysis of p(EsAzet) and p(iPsAzet) polymers prepared in DMF (DMF was used to avoid the complication of possible transfer to DMSO). Specifically, the ratios of the integration of the  $^1\text{H}$  NMR signals attributed to the terminal amide proton versus the initiator methyl group are greater than the expected 1.00:3.00 and are consistent with branched structures. For example, the ratio for p(EsAzet) and p(iPsAzet) samples ( $D_p$ 's  $\approx$  33) are 1.10:3.00 and 1.23:3.00, (Table 4 and Figures S8 and S11) respectively. A similarly prepared branched p(MsAzet) was found to have an end-group ratio of 1.04:3.00 (Table 4 and Figure S7). Therefore, the increased substitution at the alkanesulfonyl group increases branching of the resulting polymer. We propose an increase in branching is due to an increased nucleophilicity of the alkanide anion that forms upon anion transfer from the propagating chain end.

The branching in p(EsAzet) and p(iPsAzet) helps explain the improved solubility of p(EsAzet) and p(iPsAzet) (both soluble in DMF, DMSO) compared to p(tBuAzet) (insoluble in all common solvents). Since the *tert*-butylsulfonyl group of tBuAzet is not capable of the chain transfer mechanism occurring in p(EsAzet) and p(iPsAzet), p(tBuAzet) likely has a linear structure. The insolubility of p(tBuAzet) is in line with other poly(*N*-sulfonylazetidine) homopolymers and poly(*N*-sulfonylaziridine) homopolymers that lack substitution on the polymer backbone.<sup>28,31,45</sup>

## CONCLUSIONS

In summary, we report on the effect of substitution  $\alpha$  to the sulfonyl on the polymerization of *N*-(alkylsulfonyl)azetidines. The polymerizations of EsAzet and iPsAzet are of the first order with respect to the monomer, and the number of active chain ends remains constant throughout the course of the polymerization, similar to the polymerization of MsAzet. Increasing the degree of substitution on the sulfonyl with electron-donating groups plays an important role in the kinetics of polymerization. When the degree of substitution on the sulfonyl is increased, the Arrhenius activation energy of the monomers is decreased, possibly due to an increase in the nucleophilicity of the propagating aza anion. However, with increasing substitution on the sulfonyl, the Arrhenius frequency factor is decreased, likely because of an increased steric interaction between the propagating chain end and the monomer. The effects of the changes in the degree of substitution to the two Arrhenius parameters lead to changes in the ordering of the polymerization rates at different temperatures. The resulting polymers, p(EsAzet) and p(iPsAzet), contain branching due to chain transfer by activation of the sulfonyl groups on both the monomer and polymer backbone. Interestingly, the degree of branching increases with increased substitution  $\alpha$  to the sulfonyl, likely due to increased reactivity of the formed alkanide anion. The branching in p(EsAzet) and p(iPsAzet) appears to be essential for the solubility of the polymers formed as p(tBuAzet), which cannot branch, is insoluble in all common solvents. This work highlights the effects of substitution on the sulfonyl group in *N*-(alkylsulfonyl)azetidines on the kinetics and architecture of p(*N*-(alkylsulfonyl)azetidine) homopolymers, which will be further explored in future work.

## ASSOCIATED CONTENT

### S Supporting Information

The Supporting Information is available free of charge on the ACS Publications website at DOI: [10.1021/acs.macromol.9b01436](https://doi.org/10.1021/acs.macromol.9b01436).

Experimental procedures, NMR spectra, MALDI-TOF mass spectra, SEC, and thermal analysis plots (PDF)

Unprocessed experimental data can be found online via Open Science Framework at: DOI 10.17605/OSF.IO/R5EPB.

## AUTHOR INFORMATION

### Corresponding Author

\*E-mail: [parupar@ua.edu](mailto:parupar@ua.edu).

ORCID 

Louis Reisman: 0000-0003-2330-9804

Paul A. Rupar: 0000-0002-9532-116X

### Author Contributions

‡E.A.R. and L.R. contributed equally. All authors have given approval to the final version of the manuscript.

### Notes

The authors declare no competing financial interest.

### ACKNOWLEDGMENTS

We thank the ACS-Petroleum Research Fund (no. 55075-DNI7), the Department of Education-GAANN (no. P200A150329), NASA (no. 80MSFC18M0041), and the University of Alabama (UA) for financial support. We thank NSF (no. CHE-1726812) from the Major Research Instrumentation (MRI) program for purchase of the MALDI/TOF-TOF mass spectrometer.

### REFERENCES

- (1) Cationic Ring-Opening Polymerization. In *Advances in Polymer Science*; Penczek, S.; Kubisa, P.; Matyjaszewski, K., Eds.; Springer: Berlin, Heidelberg, Germany, 1985, Vol. 68/69, pp 52–65.
- (2) Gee, G.; Higginson, W. C. E.; Levesley, P.; Taylor, K. J. 266. Polymerisation of epoxides. Part I. Some kinetic aspects of the addition of alcohols to epoxides catalysed by sodium alkoxides. *J. Chem. Soc.* **1959**, 1338–1344.
- (3) Gee, G.; Higginson, W. C. E.; Merrill, G. T. 267. Polymerisation of epoxides. Part II. The polymerisation of ethylene oxide by sodium alkoxides. *J. Chem. Soc.* **1959**, 1345–1352.
- (4) Goethals, E. J.; Schacht, E. H.; Bruggeman, P.; Bossaer, P. Cationic Polymerization of Cyclic Amines. In *Ring-Opening Polymerization*; Saegusa, T.; Goethals, E. J., Eds.; ACS Symposium series; American Chemical Society: Washington, DC, 1977; Vol. 59, pp 1–12.
- (5) Jager, M.; Schubert, S.; Ochrimenko, S.; Fischer, D.; Schubert, U. S. Branched and linear poly(ethylene imine)-based conjugates: synthetic modification, characterization, and application. *Chem. Soc. Rev.* **2012**, *41*, 4755–4767.
- (6) Kobayashi, S. Ethylenimine polymers. *Prog. Polym. Sci.* **1990**, *15*, 751–823.
- (7) Schacht, E. H.; Goethals, E. J. Cationic polymerization of cyclic amines. 3. Polymerization of azetidine. *Makromol. Chem.* **1974**, *175*, 3447–3459.
- (8) Sarazen, M. L.; Jones, C. W. Insights into Azetidine Polymerization for the Preparation of Poly(propylenimine)-Based CO<sub>2</sub> Adsorbents. *Macromolecules* **2017**, *50*, 9135–9143.
- (9) Sarazen, M. L.; Sakwa-Novak, M. A.; Ping, E. W.; Jones, C. W. Effect of Different Acid Initiators on Branched Poly(propylenimine) Synthesis and CO<sub>2</sub> Sorption Performance. *ACS Sustainable Chem. Eng.* **2019**, *7*, 7338–7345.
- (10) Mees, M. A.; Hoogenboom, R. Full and partial hydrolysis of poly(2-oxazoline)s and the subsequent post-polymerization modification of the resulting polyethylenimine (co)polymers. *Polym. Chem.* **2018**, *9*, 4968–4978.
- (11) Levy, A.; Litt, M. Polymerization of cyclic imino ethers. II. Oxazines. *J. Polym. Sci., Part B: Polym. Lett.* **1967**, *5*, 881–886.
- (12) Saegusa, T.; Nagura, Y.; Kobayashi, S. Isomerization Polymerization of 1,3-Oxazine. I. Polymerization of Unsubstituted 5,6-Dihydro-4H-1,3-oxazine Giving Poly(*N*-formyltrimethylenimine) and Its Alkaline Hydrolysis of Poly(trimethylenimine). *Macromolecules* **1973**, *6*, 495–498.
- (13) Saegusa, T.; Kobayashi, S.; Nagura, Y. Isomerization Polymerization of 1,3-Oxazine. II. Kinetic Studies of the Ring-Opening Isomerization Polymerization of Unsubstituted 5,6-Dihydro-4H-1,3-oxazine. *Macromolecules* **1974**, *7*, 265–272.
- (14) Saegusa, T.; Kobayashi, S.; Nagura, Y. Isomerization Polymerization of 1,3-Oxazine. III. Kinetic Studies in the Ring-Opening Polymerization of 2-Phenyl-5,6-dihydro-4H-1,3-oxazine by Methyl Tosylate and Methyl Iodide Initiators. *Macromolecules* **1974**, *7*, 272–277.
- (15) Kobayashi, S.; Isobe, M.; Saegusa, T. Spontaneous 2:1 sequence-regulated copolymerization of cyclic imino ethers with cyclic carboxylic anhydrides. *Macromolecules* **1982**, *15*, 703–707.
- (16) Miyamoto, M.; Aoi, K.; Saegusa, T. Ring-opening polymerization of six- and seven-membered cyclic pseudoureas. *J. Polym. Sci., Part A: Polym. Chem.* **1997**, *35*, 933–945.
- (17) Kobayashi, S.; Uyama, H. Polymerization of cyclic imino ethers: From its discovery to the present state of the art. *J. Polym. Sci., Part A: Polym. Chem.* **2002**, *40*, 192–209.
- (18) Sinnwell, S.; Ritter, H. Microwave Accelerated Polymerization of 2-Phenyl-2-oxazoline. *Macromol. Rapid Commun.* **2005**, *26*, 160–163.
- (19) Sinnwell, S.; Ritter, H. Microwave Accelerated Polymerization of 2-Phenyl-5,6-dihydro-4H-1,3-oxazine: Kinetics and Influence of End-Groups on Glass Transition Temperature. *Macromol. Rapid Commun.* **2006**, *27*, 1335–1340.
- (20) Bloksma, M. M.; Schubert, U. S.; Hoogenboom, R. Poly(cyclic imino ether)s Beyond 2-Substituted-2-oxazolines. *Macromol. Rapid Commun.* **2011**, *32*, 1419–1441.
- (21) Bloksma, M. M.; Paulus, R. M.; van Kuringen, H. P. C.; van der Woerdt, F.; Lambermont-Thijs, H. M. L.; Schubert, U. S.; Hoogenboom, R. Thermoresponsive Poly(2-oxazine)s. *Macromol. Rapid Commun.* **2012**, *33*, 92–96.
- (22) Dhende, V. P.; Samanta, S.; Jones, D. M.; Hardin, I. R.; Locklin, J. One-Step Photochemical Synthesis of Permanent, Nonleaching, Ultrathin Antimicrobial Coatings for Textiles and Plastics. *ACS Appl. Mater. Interfaces* **2011**, *3*, 2830–2837.
- (23) Zou, G. F.; Zhao, J.; Luo, H. M.; McCleskey, T. M.; Burrell, A. K.; Jia, Q. X. Polymer-assisted-deposition: a chemical solution route for a wide range of materials. *Chem. Soc. Rev.* **2013**, *42*, 439–449.
- (24) Pang, S. H.; Lee, L. C.; Sakwa-Novak, M. A.; Lively, R. P.; Jones, C. W. Design of Aminopolymer Structure to Enhance Performance and Stability of CO<sub>2</sub> Sorbents: Poly(propylenimine) vs Poly(ethylenimine). *J. Am. Chem. Soc.* **2017**, *139*, 3627–3630.
- (25) Pang, S. H.; Lively, R. P.; Jones, C. W. Oxidatively-Stable Linear Poly(propylenimine)-Containing Adsorbents for CO<sub>2</sub> Capture from Ultradilute Streams. *ChemSusChem* **2018**, *11*, 2628–2637.
- (26) Sujan, A. R.; Pang, S. H.; Zhu, G.; Jones, C. W.; Lively, R. P. Direct CO<sub>2</sub> Capture from Air using Poly(ethylenimine)-Loaded Polymer/Silica Fiber Sorbents. *ACS Sustainable Chem. Eng.* **2019**, *7*, 5264–5273.
- (27) Hicks, J. C.; Drese, J. H.; Fauth, D. J.; Gray, M. L.; Qi, G.; Jones, C. W. Designing Adsorbents for CO<sub>2</sub> Capture from Flue Gas-Hyperbranched Aminosilicas Capable of Capturing CO<sub>2</sub> Reversibly. *J. Am. Chem. Soc.* **2008**, *130*, 2902–2903.
- (28) Stewart, I. C.; Lee, C. C.; Bergman, R. G.; Toste, F. D. Living Ring-Opening Polymerization of *N*-Sulfonylaziridines: Synthesis of High Molecular Weight Linear Polyamines. *J. Am. Chem. Soc.* **2005**, *127*, 17616–17617.
- (29) Homann-Müller, T.; Rieger, E.; Alkan, A.; Wurm, F. R. N-Ferrocenylsulfonyl-2-methylaziridine: the first ferrocene monomer for the anionic (co)polymerization of aziridines. *Polym. Chem.* **2016**, *7*, 5501–5506.
- (30) Rieger, E.; Manhart, A.; Wurm, F. R. Multihydroxy Polyamines by Living Anionic Polymerization of Aziridines. *ACS Macro Lett.* **2016**, *5*, 195–198.
- (31) Thomi, L.; Wurm, F. R. Aziridine Termination of Living Anionic Polymerization. *Macromol. Rapid Commun.* **2014**, *35*, 585–589.
- (32) Rieger, E.; Blankenburg, J.; Grune, E.; Wagner, M.; Landfester, K.; Wurm, F. R. Controlling the Polymer Microstructure in Anionic Polymerization by Compartmentalization. *Angew. Chem., Int. Ed.* **2018**, *57*, 2483–2487.
- (33) Gleede, T.; Rieger, E.; Blankenburg, J.; Klein, K.; Wurm, F. R. Fast Access to Amphiphilic Multiblock Architectures by the Anionic Copolymerization of Aziridines and Ethylene Oxide. *J. Am. Chem. Soc.* **2018**, *140*, 13407–13412.

(34) Rieger, E.; Alkan, A.; Manhart, A.; Wagner, M.; Wurm, F. R. Sequence-Controlled Polymers via Simultaneous Living Anionic Copolymerization of Competing Monomers. *Macromol. Rapid Commun.* **2016**, *37*, 833–839.

(35) Rieger, E.; Gleede, T.; Weber, K.; Manhart, A.; Wagner, M.; Wurm, F. R. The living anionic polymerization of activated aziridines: a systematic study of reaction conditions and kinetics. *Polym. Chem.* **2017**, *8*, 2824–2832.

(36) Thomi, L.; Wurm, F. R. Living Anionic Polymerization of Functional Aziridines. *Macromol. Symp.* **2015**, *349*, 51–56.

(37) Gleede, T.; Rieger, E.; Homann-Müller, T.; Wurm, F. R. 4-Styrenesulfonyl-(2-methyl)aziridine: The First Bivalent Aziridine-Monomer for Anionic and Radical Polymerization. *Macromol. Chem. Phys.* **2018**, *219*, 1700145.

(38) Rieger, E.; Gleede, T.; Manhart, A.; Lamla, M.; Wurm, F. R. Microwave-Assisted Desulfonylation of Polysulfonamides toward Polypropylenimine. *ACS Macro Lett.* **2018**, *7*, 598–603.

(39) Gleede, T.; Rieger, E.; Liu, L.; Bakkali-Hassani, C.; Wagner, M.; Carlotti, S.; Taton, D.; Andrienko, D.; Wurm, F. R. Alcohol- and Water-Tolerant Living Anionic Polymerization of Aziridines. *Macromolecules* **2018**, *51*, 5713–5719.

(40) Bakkali-Hassani, C.; Rieger, E.; Vignolle, J.; Wurm, F. R.; Carlotti, S.; Taton, D. The organocatalytic ring-opening polymerization of *N*-tosyl aziridines by an *N*-heterocyclic carbene. *Chem. Commun.* **2016**, *52*, 9719–9722.

(41) Bakkali-Hassani, C.; Rieger, E.; Vignolle, J.; Wurm, F. R.; Carlotti, S.; Taton, D. Expanding the scope of *N*-heterocyclic carbene-organocatalyzed ring-opening polymerization of *N*-tosyl aziridines using functional and non-activated amine initiators. *Eur. Polym. J.* **2017**, *95*, 746–755.

(42) Bakkali-Hassani, C.; Coutouly, C.; Gleede, T.; Vignolle, J.; Wurm, F. R.; Carlotti, S.; Taton, D. Selective Initiation from Unprotected Aminoalcohols for the *N*-Heterocyclic Carbene-Organocatalyzed Ring-Opening Polymerization of 2-Methyl-*N*-tosyl Aziridine: Telechelic and Block Copolymer Synthesis. *Macromolecules* **2018**, *51*, 2533–2541.

(43) Wang, X.; Liu, Y.; Li, Z.; Wang, H.; Gebru, H.; Chen, S.; Zhu, H.; Wei, F.; Guo, K. Organocatalyzed Anionic Ring-Opening Polymerizations of *N*-Sulfonyl Aziridines with Organic Superbases. *ACS Macro Lett.* **2017**, *6*, 1331–1336.

(44) Wang, Y.; Yang, R.; Luo, W.; Li, Z.; Zhang, Z.; Wu, C.; Hadjichristidis, N. 2-Azaallyl Anion Initiated Ring-Opening Polymerization of *N*-Sulfonyl Aziridines: One-Pot Synthesis of Primary Amine-Ended Telechelic Polyaziridines. *Macromolecules* **2019**, *52*, 3888–3896.

(45) Reisman, L.; Mbarushimana, C. P.; Cassidy, S. J.; Rupar, P. A. Living Anionic Copolymerization of 1-(Alkylsulfonyl)aziridines to Form Poly(sulfonylaziridine) and Linear Poly(ethylenimine). *ACS Macro Lett.* **2016**, *5*, 1137–1140.

(46) Mbarushimana, P. C.; Liang, Q.; Allred, J. M.; Rupar, P. A. Polymerizations of Nitrophenylsulfonyl-Activated Aziridines. *Macromolecules* **2018**, *51*, 977–983.

(47) Gleede, T.; Reisman, L.; Rieger, E.; Mbarushimana, P. C.; Rupar, P. A.; Wurm, F. R. Aziridines and Azetidines: Building Blocks for Polyamines by Anionic and Cationic Ring-Opening Polymerization. *Polym. Chem.* **2019**, *10*, 3257–3283.

(48) Reisman, L.; Rowe, E. A.; Liang, Q.; Rupar, P. A. The anionic ring-opening polymerization of *N*-(methanesulfonyl)azetidine. *Polym. Chem.* **2018**, *9*, 1618–1625.

(49) Corey, E. J.; Chaykovsky, M. Methylsulfinyl Carbanion ( $\text{CH}_3\text{SO}-\text{CH}_2^-$ ). Formation and Applications to Organic Synthesis. *J. Am. Chem. Soc.* **1965**, *87*, 1345–1353.

(50) Reisman, L.; Rowe, E. A.; Jackson, E. M.; Thomas, C.; Simone, T.; Rupar, P. A. Anionic Ring-Opening Polymerization of *N*-(tolylsulfonyl)azetidines To Produce Linear Poly(trimethylenimine) and Closed-System Block Copolymers. *J. Am. Chem. Soc.* **2018**, *140*, 15626–15630.

(51) Sun, P.; Weinreb, S. M.; Shang, M. tert-Butylsulfonyl (Bus), a New Protecting Group for Amines. *J. Org. Chem.* **1997**, *62*, 8604–8608.

(52) Tan, S.; Chen, Y.; Zingaro, R. A.; Reibenspies, J. H. Synthesis and characterization of *N*-arylsulfonylazetidines. *J. Heterocycl. Chem.* **2008**, *45*, 1229–1232.

(53) The reaction being first order with respect to [I] for EsAzet and iPsAzet polymerizations is a valid assumption based on the AROP of MsAzet.

(54) Price, C. C. Polyethers. *Acc. Chem. Res.* **1974**, *7*, 294–301.